International Journal of Modern Physics B
© World Scientific Publishing Company

VANISHING HALL AND LONGITUDINAL RESISTANCES IN BILAYER TWO-DIMENSIONAL ELECTRON SYSTEMS AT $\nu_T = 1$

MELINDA KELLOGG AND JAMES P. EISENSTEIN*

Condensed Matter Physics, California Institute of Technology, Pasadena, California 91125, USA

LOREN N. PFEIFFER AND KENNETH W. WEST

Bell Laboratories, Lucent Technologies Murray Hill, New Jersey 07974, USA

Received DAY MONTH YEAR
Revised DAY MONTH YEAR

Longitudinal and Hall resistances have been measured in a bilayer two-dimensional electron system at $\nu_T = 1$ with equal but oppositely directed currents flowing in the two layers. In the limit of zero temperature, both of these resistances are observed to drop to zero. This supports the prediction of an excitonic superfluid state existing at this total filling factor.

Keywords: counterflow superfluidity; quantum Hall effect

1. Introduction

Superfluidity has been predicted to exist in bilayer two-dimensional electron systems (2DES) provided that the layers are sufficiently close together.[1,2,3,4] Recent experiments given indirect evidence of this superfluid mode in the form of Josephson-like interlayer tunneling[5] and Hall drag[6]. In this paper we present direct evidence of superfluid flow of counterflowing currents in a bilayer electron system.

In a strong perpendicular magnetic field a single layer 2DES displays the integer and fractional quantum Hall effect (QHE) in response to the single particle and many-body energy gaps that develop in the density of states. In a bilayer system, when the layers are brought sufficiently close together, new states are seen that have no counterpart in a single layer[7,8]. In particular, when each layer is at filling factor $\nu = \frac{1}{2}$ (the lowest Landau level in each layer is half-filled), the bilayer system as a whole will exhibit a QHE — while a single layer at $\nu = \frac{1}{2}$ does not show a QHE. This indicates that a uniquely bilayer energy gap has formed in the density of states.

*corresponding author: jpe@caltech.edu

In systems where there is significant interlayer tunneling, this gap is largely due to the tunneling gap energy Δ_{SAS}: the energy difference between the lowest energy symmetric state and antisymmetric state in the double quantum well system. However, this bilayer QHE has been observed even when Δ_{SAS} is much smaller than any other energy scale in the system[5,6,9]. Theoretically, many-body effects involving the electrons in both layers will produce an energy gap even in the absence of tunneling. This state, characterized by an energy gap for charged excitations in conjunction with a neutral linearly dispersing gapless mode, can be equivalently described as a quantum Hall ferromagnet, a condensate of composite bosons, or as an excitonic condensate where electrons in one layer form Cooper pairs with 'holes' in the other[1,3,4,10]. This state is expected to display superfluid properties as has recently been supported by the observations of Josephson-like interlayer tunneling[5,11] and Hall drag[6].

This predicted superfluid mode shows itself as equal but oppositely directed currents flowing through the two layers without dissipation or motive force, thus with infinite conductivity. We have set up this current configuration, which we call "counterflow", in order to directly measure the resistivity matrix of these currents. By inverting the resistivity matrix, we find that the conductivity increases dramatically as the temperature is lowered, supporting the superfluid model.

2. Experimental Details

These experiments were performed on modulation-doped GaAs/AlGaAs double quantum wells grown by molecular beam epitaxy. Two GaAs wells 18nm wide are separated by a 10nm wide $Al_{0.9}Ga_{0.1}As$ barrier, giving a center-to-center well separation $d = 28$ nm. Using standard photolithography techniques, we etched a 160μm x 320μm mesa with 7 arms extending out from it (see Figure 1). AuNiGe contacts diffused into the ends of each arm provide electrical contact to the 2DES. Electrostatic aluminum gates above and below the arms are used to control which layer the contacts are connected to.[12] Arms 1, 2, 3 and 4 make up the two "Y"-shaped projections at the opposite ends of the bar and are used for injecting current symmetrically into the layers; arms 5, 6 and 7 are for probing the longitudinal and Hall voltages in the main mesa region. The longitudinal probes (5, 6) are spaced 160μm apart, this is equal to the width of the mesa and so we are meausuring along "one square". The as-grown electron density is $5.4 \times 10^{10}\text{cm}^{-2}$ per layer and the mobility is approximately $1 \times 10^{6}\text{cm}^2/\text{Vs}$. We can vary the density *in situ* with large aluminum gates evaporated above and below the central mesa area. The sample was thinned to 49μm.

The tunneling gap energy for this system is calculated to be $\Delta_{SAS} \approx 90$ μK — much smaller than the other energy scales in the system: temperature (≈ 30 mK), cyclotron energy (≈ 40 K) and Coulomb energy (≈ 70 K). It is also much smaller than the observed transport gap for the bilayer QHE (≈ 0.5 K, see Sec. 3.2). So we are working in the regime $\Delta_{SAS} \to 0$. The tunneling resistance measured at

resonance in zero magnetic field is $\approx 100\text{M}\Omega$.

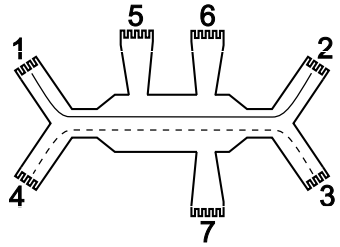

Fig. 1. A schematic illustration of the mesa region: arms 1-4 are for driving currents through the electron layers and arms 5-7 are for measuring the resulting voltages. For the counterflow configuration, a current is sent through the bottom layer by arms 1 and 2 (the solid line shows the route) and then an oppositely directed current goes through the top layer through arms 3 and 4 (the dashed line).

For the measurements shown here, a 2.3 Hz, 0.5 nA current is sent first through one of the layers, taken out, and then sent through the other layer going either in the same direction (the parallel configuration) or in the opposite direction (the counterflow configuration). Because the bilayer quantum Hall $\nu_T = 1$ state exhibits enhanced tunneling, we can indirectly detect this by measuring the current before it enters the first layer and then after it has left the first layer but before entering the second layer; the difference between the two is the tunneling current. We measure a ≈ 5 pA difference when the system is at $\nu_T = 1$. In the counterflow configuration, this will not affect the relative magnitudes of the currents in the layers, they will still carry equal but opposite currents despite the small tunneling leakage.

We measure the voltages in just one of the layers. The longitudinal (Hall) voltage V_{xx} (V_{xy}) divided by the injected current, yields the longitudinal (Hall) resistance R_{xx} (R_{xy}). Superscripts $\parallel$ and CF indicate whether the current configuration was parallel or counterflow respectively.

3. Data

3.1. *Hall and Longitudinal Resistance — Parallel versus Counterflow*

Figure 2 shows the primary result of this experiment. The main figure shows the Hall resistance for constant density $n = 2.46 \times 10^{10}$ cm^{-2} per layer, as the magnetic field is ramped from zero to 2.4T, at T =0.03 K, for both the parallel (dotted line) and counterflow (solid line) configurations. This density corresponds to d/ℓ=1.55 when calculated at $\nu_T = 1$, where $\ell = (\hbar/eB)^{1/2}$ is the magnetic length. The ratio d/ℓ is called the effective layer separation and characterizes the relative importance of the inter- versus intra- layer Coulomb interactions.

Up to about 1.8T the layers behave independently and we see the usual quantum

Hall effect as though the second layer were non-existent. The direction of the current in the second layer is irrelevant and so $R_{xy}^{\parallel} = R_{xy}^{CF}$. But as the system enters the highly correlated bilayer quantum Hall state at $\nu_T = 1$, centered around 2T, the direction of the current in the second layer splits the data: $R_{xy}^{\parallel}$ goes up to form a quantized plateau at $2h/e^2$ while R_{xy}^{CF} drops to zero. Notice that the plateau in the parallel configuration is at twice the expected value for total filling factor one, this is because we define the resistance as the voltage divided by the current in a single layer, not the net current flowing through the bilayer.

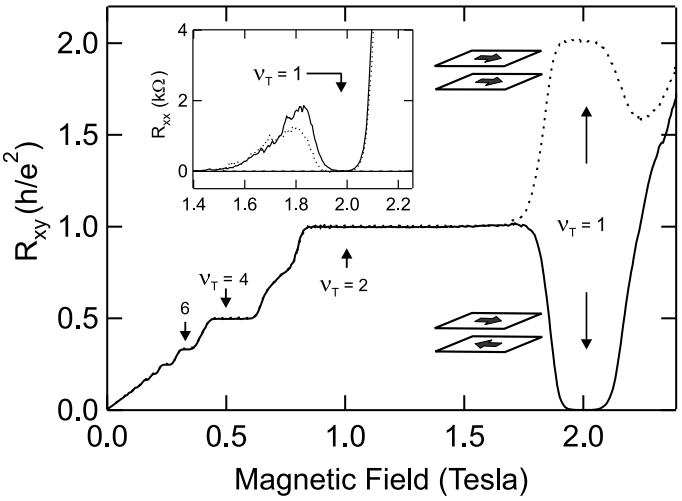

Fig. 2. Main figure shows the Hall resistivity versus magnetic field in the parallel (dotted line) and counterflow (solid line) configuration for $n = 2.46 \times 10^{10}$ cm^{-2} and T =30 mK. The inset shows the longitudinal resistances. Voltages are measured in one layer only.

The inset shows the longitudinal resistances $R_{xx}^{\parallel}$ and R_{xx}^{CF} under the same conditions, here just focusing on the region near $\nu_T = 1$. Although not shown, the two are again identical at low fields. And unlike the Hall resistance, they are also nearly identical in the interlayer coherent state at $\nu_T = 1$. R_{xx}^{CF} (solid line) is a little larger than $R_{xx}^{\parallel}$ (dotted line) around 1.8T, which is where the sample is transitioning into the $\nu_T = 1$ state. This is because of the strong interlayer Coulomb drag that occurs in the transition region.[13] When the sample is in the counterflow configuration, the two oppositely directed currents will exert a strong dragging force on one another that does not exist in the parallel configuration, and so R_{xx}^{CF} will be increased over the parallel value $R_{xx}^{\parallel}$. As both $R_{xx}^{\parallel}$ and R_{xx}^{CF} go to zero at $\nu_T = 1$, this indicates that the $\nu_T = 1$ state is dissipationless in both the parallel and counterflow configurations.

3.2. *Temperature Dependence at $\nu_T = 1$*

Focusing on the resistances at $\nu_T = 1$ only, Figure 3 shows the temperature dependence of the various quantities when the system is in the interlayer coherent state. Panel a shows $R^{\parallel}_{xx}$ (open circles) and $R^{\parallel}_{xy}$ (closed squares) for d/ℓ=1.48 for temperatures ranging from 35 mK to 400 mK. The Hall resistance never strays far from its quantized value $2h/e^2$, while the longitudinal resistance drops almost 3 orders of magnitude over this temperature range, exhibiting straight line activated behavior $R^{\parallel}_{xx} = R_0 e^{-\Delta/2T}$ with energy gap $\Delta \approx 0.5$ K.

Panel b shows the same for the counterflow resistances, R^{CF}_{xx} (open circles) and R^{CF}_{xy} (closed squares). R^{CF}_{xx} is very similar to $R^{\parallel}_{xx}$; showing the same activated behavior with the same energy gap of 0.5 K. But here R^{CF}_{xy} also drops precipitously as the temperature is lowered and at a very similar rate to both the R_{xx} data, though it does not form a straight line as the others do.

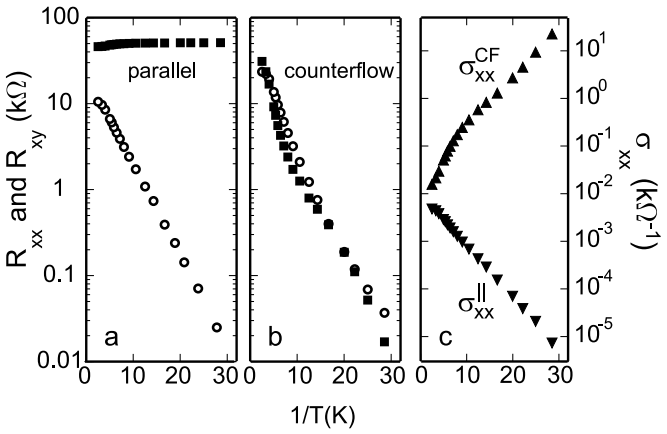

Fig. 3. Temperature dependence of the resistances (panels a and b) and conductivity (panel c) at $\nu_T = 1$ for both parallel and counterflow configurations at d/ℓ =1.48. In a) open circles represent $R^{\parallel}_{xx}$, closed squares $R^{\parallel}_{xy}$; in b) open circles represent R^{CF}_{xx}, closed squares R^{CF}_{xy}. c) shows the counterflow and parallel longitudinal conductivities, σ^{CF}_{xx} and $\sigma^{\parallel}_{xx}$, respectively.

More illuminating is the same data plotted as longitudinal conductivity $\sigma_{xx} = \rho_{xx}/(\rho^2_{xx}+\rho^2_{xy})$ shown in panel c.[14] Here the transport properties of the two different current configurations clearly and radically diverge as the temperature is lowered. The upward pointing triangles in the top half of panel c indicate the longitudinal conductivity in the counterflow configuration σ^{CF}_{xx}; and the downward triangles in the bottom half represent $\sigma^{\parallel}_{xx}$. $\sigma^{\parallel}_{xx}$ goes to zero as the temperature goes to zero, again, in an activated fashion. This is precisely the behavior expected for any ordinary quantum Hall state. On the other hand, σ^{CF}_{xx} becomes dramatically larger as T is lowered. By 35 mK there are more than six orders of magnitude difference in the conductivities of the two current configurations. This behavior of σ^{CF}_{xx} is

completely novel, indicating superfluid flow in the zero temperature limit.

3.3. *Dependence on Effective Layer Separation d/ℓ*

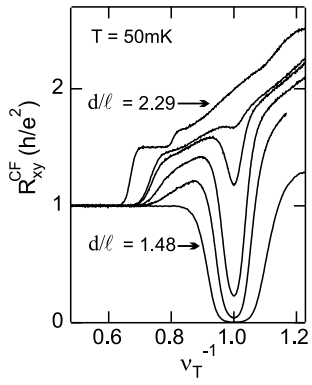

Fig. 4. Sample enters excitonic superfluid state as evidenced by R_{xy}^{CF} dropping to zero as the effective layer separation d/ℓ is reduced. Figure shows R_{xy}^{CF} versus inverse filling factor ν_T^{-1} for d/ℓ = 2.29, 1.75, 1.71, 1.66, 1.59, 1.48, all at $T = 50$ mK.

Figure 4 shows the dependence on the effective layer separation d/ℓ, looking at just R_{xy}^{CF} as the indicator of the onset of the bilayer quantum Hall state. R_{xy}^{CF} is plotted versus the inverse of the total filling factor $\nu_T^{-1} = eB/hn_T$ (for easier comparison of data with different d/ℓ) taken at T =50 mK. The topmost curve, with d/ℓ=2.29, shows the sample to be well out of the interlayer coherent state. The behavior seen is typical of the Hall resistance in a single layer 2DES. There is no distortion or feature at $\nu_T = 1$, indicating a lack of correlation with the second layer. As d/ℓ is reduced, a dip begins to form at $\nu_T = 1$, becoming deeper and more fully developed as the layers are brought (effectively) closer together. By d/ℓ=1.48 there is a broad minimum that goes nearly to zero signaling that the sample is now well within the bilayer quantum Hall state. By interpolation, the minimum reaches half its uncorrelated value when it's at d/ℓ=1.70, which may be thought of as the location of the phase boundary. This is consistent with observations of the phase boundary location as measured in prior Coulomb drag experiments.[13]

4. Discussion

The view of this state as a Bose-Einstein condensate of interlayer excitons[4] offers the most intuitively accessible explanation of our observations, and so we focus on this interpretation. In this view one of the half-filled Landau levels in the individual layers can alternately be viewed as a full Landau level that is half-filled with holes. This state is characterized by the electrons in one layer forming Cooper pairs with

the holes in the other layer and condensing into a superfluid (see Fig. 5). Counterflow superfluidity can then be thought of as dissipationless uniform flow of these excitons in one direction, creating oppositely directed currents in the two layers.

A key feature of this state, besides it being dissipationless, is that the counterflowing currents are being carried by *charge-neutral* particles. Charge-neutral particles will not be affected by the magnetic field and so will not produce a Hall voltage. This prediction is spectacularly confirmed by the vanishing Hall voltage at $\nu_T = 1$ shown in Fig. 2.

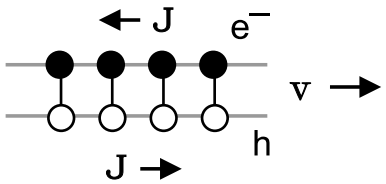

Fig. 5. Schematic showing how interlayer excitons can create counterflowing currents in the two layers. Electrons (e^-) in one layer bind to conduction band holes (h) in the other layer, and the resulting excitons condense into a superfluid. Dissipationless flow in one direction produces equal but oppositely directed dissipationless currents (**J**) in the layers.

However, as Fig. 3 shows, both the dissipation R_{xx}^{CF} and Hall resistivity R_{xy}^{CF} in the counterflow configuration remain finite at finite temperatures. In the ideal case, both of these quantities should drop to zero for $T < T_{KT}$, where T_{KT} is the Kosterlitz-Thouless temperature.[15] Instead we find activated behavior. One reason for this activated behavior is that the critical current for this superfluid is zero, so the act of making a resistance measurement at all will impart an energy gap to the system. However, this energy gap should be dependent on the magnitude of the current. Our observed energy gap of $\Delta \approx 0.5$ K persists even when we use different drive currents (from 20 pA to 1 nA).

The presence of interlayer tunneling in the sample, even though extremely small, also disturbs the state. The binding of neutral vortex-antivortex excitations is a crucial element of the Kosterlitz-Thouless phase transition. Tunneling alters the binding of these pairs, and if the tunneling is strong enough, it binds *charged* vortex-antivortex pairs, creating an energy gap for these new charged excitations.[16]

Or we may be seeing an energy gap due to disorder in the system. The sample is going insulating at magnetic fields just above $\nu_T = 1$ (see inset of Fig. 2). Thus we are working in a regime where disorder effects are strong. There may be free vortices in our sample that are caused by the disorder, and not the current, and we are measuring some activation energy associated with hopping from disorder site to disorder site. Alternately, the combination of finite tunneling in a strong enough disorder potential can create strings of overturned spins with free vortices at either end, with possible low energy excitations of the vortices and the creation of new

"string glass" states.[17]

5. CONCLUSIONS

We have observed vanishing Hall and longitudinal resistances in the counterflow current configuration of a bilayer two-dimensional electron system at $\nu_T = 1$. The conductivity in the counterflow channel increases dramatically as the temperature is reduced. Contrariwise, the transport coefficients in the parallel channel exhibit the ordinary quantum Hall effect, both $R_{xx}^{\parallel}$ and $\sigma_{xx}^{\parallel}$ go to zero in an activated manner as the temperature goes to zero. These observations are consistent with a model of this state as a Bose-Einstein condensate of excitons, though we are uncertain as to the origin of the $\Delta \approx 0.5$ K energy gap.

Acknowledgements

We wish to thank A.H. MacDonald, S.M. Girvin, Z. Wang and D.N. Sheng for helpful discussions. This work was supported by the NSF under Grant No. DMR-0242946 and the DOE under Grant No. DE-FG03-99ER45766.

References

1. X.G. Wen and A. Zee, *Phys. Rev. Lett.* **69**, 1811 (1992).
2. Z.F. Ezawa and A. Iwazaki, *Phys. Rev.* **B47**, 7295 (1993).
3. K. Moon, *et al.*, *Phys. Rev.* **B51**, 5138 (1995).
4. A.H. MacDonald, *Physica* **B298**, 129 (2001).
5. I.B. Spielman, J.P. Eisenstein, L.N. Pfeiffer, and K.W. West, *Phys. Rev. Lett.* **84**, 5808 (2000).
6. M. Kellogg, I.B. Spielman, J.P. Eisenstein, L.N. Pfeiffer, and K.W. West, *Phys. Rev. Lett.* **88**, 126804 (2002).
7. J.P. Eisenstein, G.S. Boebinger, L.N. Pfeiffer, K.W. West, and S. He, *Phys. Rev. Lett.* **68**, 1383 (1992).
8. Y.W. Suen, L.W. Engel, M.B. Santos, M. Shayegan, and D.C. Tsui, *Phys. Rev. Lett.* **68**, 1379 (1992).
9. S.Q. Murphy, J.P. Eisenstein, G.S. Boebinger, L.N. Pfeiffer, and K.W. West, *Phys. Rev. Lett.* **72**, 728 (1994).
10. K. Yang, *et al.*, *Phys. Rev. Lett.* **72**, 732 (1994).
11. I.B. Spielman, J.P. Eisenstein, L.N. Pfeiffer, and K.W. West, *Phys. Rev. Lett.* **87**, 036803 (2001).
12. J.P. Eisenstein, L.N. Pfeiffer, and K.W. West, *Appl. Phys. Lett.* **57**, 2324 (1990).
13. M. Kellogg, J.P. Eisenstein, L.N. Pfeiffer, and K.W. West, *Phys. Rev. Lett.* **90**, 246801 (2003).
14. We take $\rho = R$ as the longitudinal voltage probes are spaced one square apart.
15. J.M. Kosterlitz and D.J. Thouless, *J. Phys.* **C6**, 1181 (1973).
16. See the chapter by S.M. Girvin and A.H. MacDonald in *Perspectives in Quantum Hall Effects*, edited by S. Das Sarma and A. Pinczuk (John Wiley & Sons, Inc., New York, 1997).
17. H.A. Fertig and J.P. Straley, *Phys. Rev. Lett.* **91**, 046806 (2003).